

A Circularly Polarized Substrate Integrated Waveguide Antenna of Dual-Band Dual-Sense type

Dr.Pravat Kumar Subudhi¹, Ipsita Samal²

¹Professor, Department of Electronics and Communication Engineering, Gandhi Institute For Technology (GIFT), Bhubaneswar

²Assistant Professor, Department of Electronics and Communication Engineering, Gandhi Engineering College, Bhubaneswar

,Professor, Engineering, GIFT, Bhubaneswar ,GEC,Bhubaneswar

ABSTRACT—A dual-band dual-sense circularly polarized (CP) antenna is presented in substrate integrated waveguide technology. The proposed antenna consists of four V-shaped asymmetrical resonators that are placed on a circular substrate symmetrically with respect to its center. The antenna is excited by a probe on the central axis. A dual-band CP antenna is designed and fabricated. The antenna provides left-hand circular polarization (LHCP) in the lower band and right-hand circular polarization (RHCP) in the upper band. Total size of the antenna is 1963.5mm^2 on a 0.787mm thick RT/Duroid 5880 substrate. Measured axial ratios are below 3dB over $8.78\text{--}8.90\text{GHz}$ and $9.52\text{--}9.66\text{GHz}$. Over the bands, the return loss is more than 10dB . Measured cross-polarization levels are 31.1 and 24.65dB , and front-to-back ratios are 14.93 and 18.35dB over the LHCP and RHCP bands, respectively. Depending on application requirements, the band ratio can be tuned. Also, the sense of polarization can be interchanged. The antenna does not use any ground plane perturbation. Thus, it can be directly attached to a micro wave circuit.

Index Terms—Circularly polarized (CP) antenna, dual-band, dual-sense, substrate integrated waveguide (SIW).

I. INTRODUCTION

Circularly polarized (CP) antennas are popular due to their capability to avoid adverse effects caused by Faraday rotation, multipath propagation, and polarization mismatch due to misalignments between transmitting and receiving antennas. Printed CP antennas are preferred as they have low profile, low cost, and ease of fabrication [1], [2]. Dual-band CP antennas [3], [4] minimize the requirement of using two antennas for two bands. Moreover, extra features of polarization diversity can be incorporated in dual-band antennas by keeping polarization of two bands opposite to each other. Recently, many dual-band, dual-sense CP antennas are reported [5]–[11]. However, most of them provide bidirectional radiation patterns. Also, the tunability of the bands is not shown in [5]–[8] and [10]. Good radiation characteristics in low-profile antennas can be obtained when antennas are designed in substrate integrated waveguide (SIW). SIW-based linearly polarized antennas are reported in

Manuscript received January 19, 2018; accepted January 29, 2018. Date of publication January 31, 2018; date of current version March 1, 2018. (Corresponding author: Kundan Kumar.)

K. Kumar and S. Dwari are with the Department of Electronics Engineering, Indian Institute of Technology (Indian School of Mines), Dhanbad 826004, India (e-mail: kundansingh.singh5@gmail.com; sdwari@gmail.com).

M. K. Mandal is with the Department of Electronics and Electrical Communication Engineering, Indian Institute of Technology, Kharagpur 721302, India (e-mail: mkmandal@ece.iitkgp.ernet.in). Digital Object Identifier 10.1109/LAWP.2018.2800295

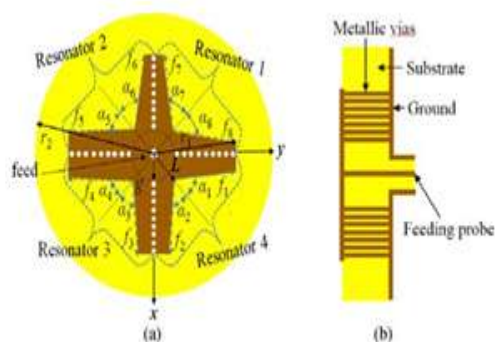


Fig. 1. Geometry of basic dual-band dual-sense antenna. (a) Top view and (b) side view. ($\alpha_1 = 47.7$, $\alpha_2 = 49.67$, $\alpha_3 = 51.2$, $\alpha_4 = 45$, $\alpha_5 = 50.2$, $\alpha_6 = 57.8$, $\alpha_7 = 57.8$, $\alpha_8 = 60.25$; unit: degrees), ($f_1 = 12.85$, $f_2 = 13.0$, $f_3 = 13.13$, $f_4 = 12.65$, $f_5 = 13.0$, $f_6 = f_7 = 13.71$, $f_8 = 13.95$, $r_1 = 19$, $r_2 = 25$, $g = 4.0$, $L = 8.48$; unit: millimeters).

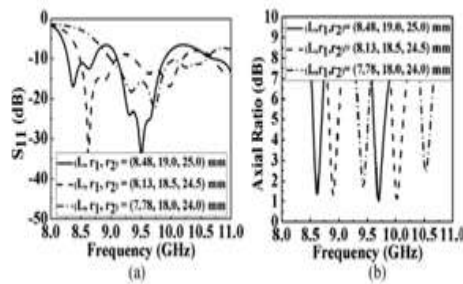


Fig. 2. Simulated (a) S_{11} and (b) axial ratio of the basic antenna. LHCP and RHCP are obtained in the lower and upper bands, respectively.

[12] and [13]. Single-band and dual-band CP SIW antennas are proposed in [14]–[17].

TABLE I DIFFERENT DUAL-BAND CP ANTENNAS WITH DIFFERENT FLARE ANGLES

	Flare angle (degree)								Frequency band and polarization state	
	α_1	α_2	α_3	α_4	α_5	α_6	α_7	α_8	Lower band	Upper band
Ant 1	47.7	49.7	51.2	45	50.2	57.8	57.8	60.25	(8.56–8.66) GHz LHCP	(9.64–9.76) GHz RHCP
Ant 2	45	51.2	49.7	47.7	50.2	57.8	57.8	60.25	(8.54–8.62) GHz RHCP	(9.51–9.68) GHz RHCP
Ant 3	47.7	49.7	51.2	45	60.25	57.8	57.8	50.2	(8.55–8.63) GHz LHCP	(9.51–9.69) GHz LHCP
Ant 4	45	51.2	49.7	47.7	60.25	57.8	57.8	50.2	(8.53–8.64) GHz RHCP	(9.61–9.75) GHz LHCP

II. DESIGN AND ANALYSIS

The configuration of the basic dual-band dual-sense CP antenna is shown in Fig. 1. The antenna is designed on a single-layer circular substrate, Roger RT/Duroid 5880 having relative permittivity of 2.2, loss tangent of 0.0009, and thickness of 0.787 mm. Four asymmetric V-shape resonators are placed symmetrically with respect to a central feeding probe. Four electrical walls realized by a set of metallic vias connect them side-by-side. For the electric walls, periodicity $p=1.5$ mm and via diameter $d=1.0$ mm. The optimized dimensions of the antenna to obtain CP radiation at 8.6 and 9.7 GHz with opposite sense of polarization are given in Fig. 1. The ground plane radius r_2 has an impact on axial ratio. A minimum substrate size must be maintained. For this example, a minimum $r_2=22$ mm behaves as an infinite ground plane, and good axial ratios are obtained. It starts to degrade below this value. The antenna characteristics and performances are investigated and analyzed by electromagnetic simulation software Ansoft HFSS.

Design of the antenna starts with $L = \lambda_0/4$ and $r_1 - g/2 = \lambda_0/2$ at the center of lower CP band. Resonant frequencies of resonators 1 and 2 are close to each other, and their dimensions L , r_1 , r_2 , α_5 , α_6 , α_7 , and α_8 determine the frequency of upper radiating band. Similarly, resonators 3 and 4 are tuned for the lower operating band. Fig. 2

However, the CP antennas in [16] and [17] have the same sense of polarization in both the bands.

In this letter, a novel dual-band dual-sense antenna is presented in SIW technology. The proposed antenna has high front-to-back ratio and low cross-polarization level. The antenna is realized on a single-layer substrate and supported by an unperturbed ground plane. Thus, it can be directly attached to a micro-wave circuit. Moreover, the band position can be controlled independently. The polarization of any band can be changed simply by changing dimensions of the resonators. To the best of the authors' knowledge, this is the first dual-band dual-sense CP antenna that uses SIW technology to obtain improved performances.

shows the variation of input matching and the CP bands with resonator dimensions. Other dimensions are kept fixed as shown in Fig. 1.

As shown in Table I, sense of polarization can be controlled by the flare angles $\alpha_{n(n=1-8)}$. Among the antennas listed in the table, Ant 1 is the basic antenna shown in Fig. 1. Ant 2 is obtained by interchanging the values of α_1 and α_4 , and those of α_2 and α_3 of Ant 1. As a result, right-hand circular polarization (RHCP) is obtained at the lower band. Similarly for Ant 3, interchanging α_5 and α_8 , and α_6 and α_7 , of Ant 1 provides left-hand circular polarization (LHCP) at the upper band. Ant 4 is obtained by interchanging flare angles between resonators 1 and 2, and resonators 3 and 4, of Ant 1. Thus, its sense of polarizations of the CP bands is opposite to Ant 1.

However, the antenna Ant 1 in Fig. 1 provides lower gain at the upper band, typically 0 dB. It is observed that a set of horizontal metallic vias, as shown in Fig. 3, improves the gain at least by 2.2 dB. In the figure, the offset $L_v=2$ mm. This modification affects the overall surface current distributions on the structure. Fig. 4 compares the antenna characteristics with and without the horizontal vias. Fig. 4(d) shows high current densities on the patch at the lower side of resonators 3 and 4, which is responsible for lowering the gain at the upper band.



Fig. 3. Modified antenna with horizontal vias at bottom.

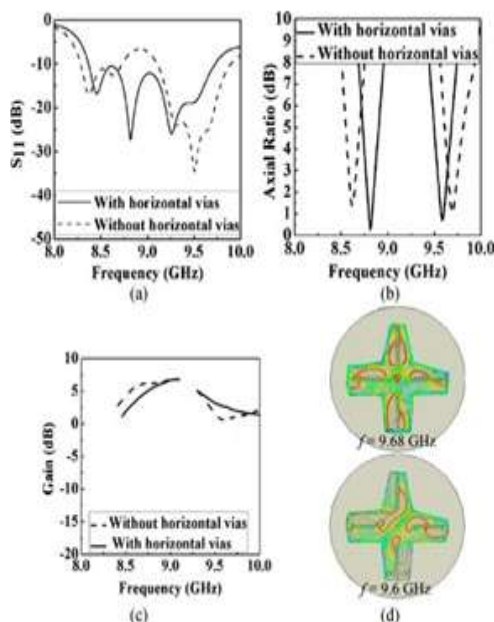


Fig. 4. Simulated (a) S_{11} (dB), (b) axial ratio, (c) broadside gains, and (d) surface current density distributions with and without the horizontal vias.

Because radiation in the upperband is obtained from resonators 1 and 2, the undesired current densities could not be decreased just by tuning resonator dimensions. A set of horizontal vias reduces the current densities and improves the gain.

Simulated fringing electric fields of the antenna at 8.82GHz at two time instances with 90° phase difference are shown in Fig. 5(a). The same at 9.6 GHz is illustrated in Fig. 5(b). It is observed that at 8.82 GHz, rotation of dominant component of electric fields with time is in clockwise direction. The V-shaped apertures of resonators 3 and 4 are excited in such a fashion that the fringing electric fields duet other resonators have equal magnitude with $+90^\circ$ phase difference. Thus, LHC is obtained. Conversely, it is in anti clock wise direction for resonators 1 and 2 providing RHC at 9.6 GHz. Variation of α_1 changes the ratio of

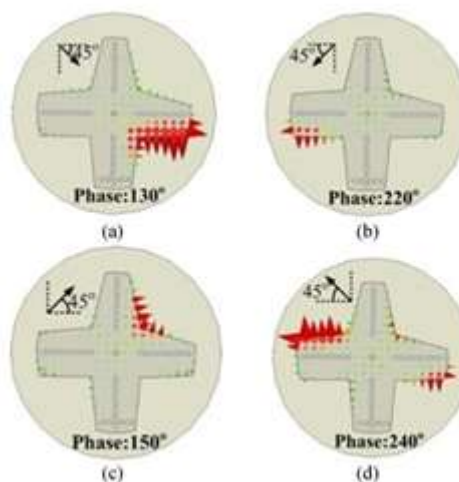


Fig. 5. Electric field distribution at: (a) 8.82 and (b) 9.6 GHz.

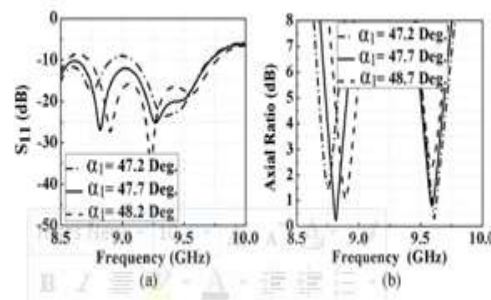


Fig. 6. Effects of different values of α_1 on (a) $|S_{11}|$ and (b) axial ratio.

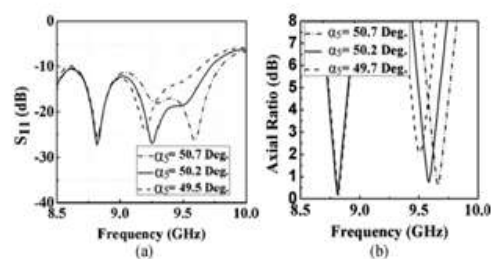


Fig. 7. Effects of different values of α_5 on (a) $|S_{11}|$ (dB) and (b) axial ratio.

horizontal to vertical components of the fringing electric fields of resonator 4. Thus, the lower CP band position changes. As an example, effects of α_1 on antenna performances are shown in Fig. 6. Similarly, as shown in Fig. 7, the upper band can be tuned by varying α_5 of resonator 2. In both cases, one band is tuned, keeping the other band almost intact.

Fig. 8 shows vector electric field distribution on the cross-sectional plane AA¹ in Fig. 3 is like the TE₁₀ mode in a half mode SIW.

III. EXPERIMENTAL RESULTS

Antenna Ant 1 is fabricated. Fig.9 shows a photograph. The simulated and measured $|S_{11}|$ of the antenna is shown in Fig.10.

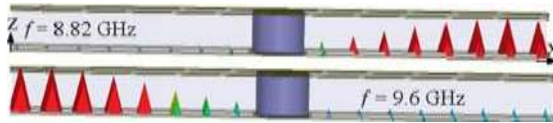


Fig. 8. Cross-sectional view of vector E-field distribution at AA¹ of Fig. 3.

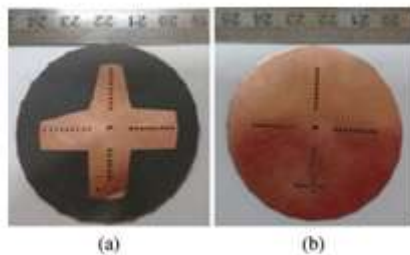


Fig. 9. Photograph of the fabricated antenna. (a) Top view. (b) Bottom view.

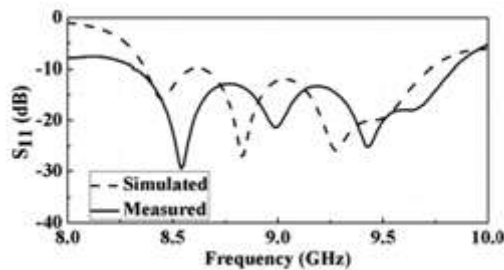


Fig. 10. Simulated and measured $|S_{11}|$ of the proposed antenna.

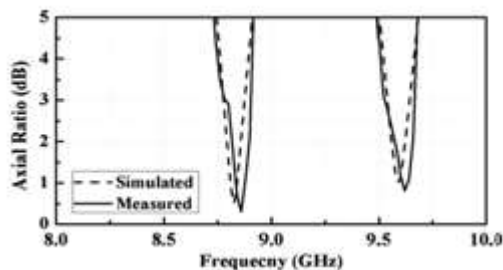


Fig. 11. Simulated and measured axial ratio of the proposed antenna.

Measured 10 dB Banded bandwidth covers both the bands from 8.32 to 9.83 GHz, which covers both the bands. The simulated and measured axial ratios are shown in Fig. 11. The 3 dB LHCP axial-ratio bandwidth at the lower band is 1.35% (8.78–8.90 GHz), and RHCP axial-ratio bandwidth at the upper band is 1.45% (9.52–

9.66 GHz). As shown in Fig. 12, the measured LHCP and RHCP gains vary from 5 to 5.8 dB and 2.7 to 4 dB, respectively.

The measured efficiency is more than 92% over both the bands. The radiation patterns are shown in Fig. 13. It is observed from the patterns that the antenna radiates LHCP wave at the lower band and RHCP wave at the upper band. The cross-polarization levels are 31.1 and 24.65 dB in the broad side direction at the lower and upper bands, respectively. Also, the antenna has directive radiation pattern with high front-to-back ratio of 14.93 and 18.35 dB at the bands, respectively. Its measured CP beam widths in

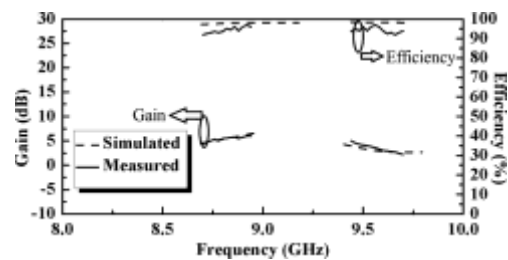


Fig. 12. Simulated and measured gains and efficiencies of the antenna.

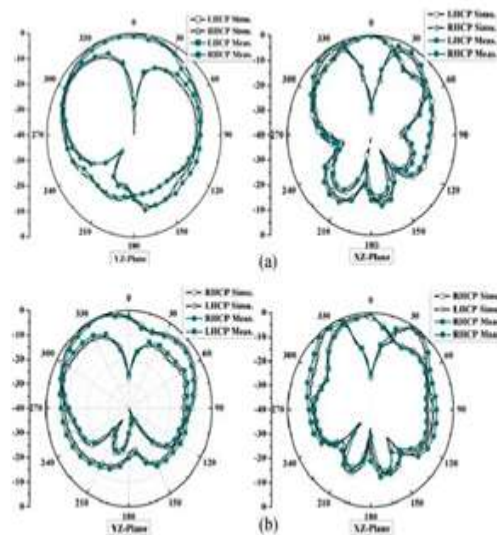


Fig. 13. Simulated and measured radiation patterns at (a) 8.82 and (b) 9.6 GHz.

TABLE II PERFORMANCE COMPARISON WITH DUAL-BAND CP SIW ANTENNAS

Parameters	[15]	[16]		[17]		This work	
	f_1	f_1	f_2	f_1	f_2	f_1	f_2
Freq.(GHz)	12.5	9.5	11.8	37.5	47.8	8.82	9.6
ARBW(%)	11.2	8	5	1.1	1.5	1.35	1.4
CP state	LH/RH	LH	LH	LH	LH	LH	RH
Size(λ^2)	0.982	2.679		1.875		1.605	
Independent tunability	NR	NR		NR		Yes	
Design flexibility	NR	NR		NR		Yes	

NR = Not reported, LH = Left-hand, RH = Right-hand.

yz plane are 19° (lower band) and 15° (upper band). The respective values in xz plane are 20° and 14° .

IV. CONCLUSION

A dual-band dual-sense probe-fed CP antenna with metallic vias is presented in printed circuit board technology. The antenna is realized on a single-layer substrate and supported by an unperturbed ground plane. The antenna is composed of four asymmetrical resonators with V-shaped apertures. Asymmetry creates two orthogonal modes having 90° phase difference at the bands of interest. Any one of the CP bands can be tuned independently keeping the other one almost fixed. The antenna has good radiation characteristics. In Table II, performance of the present antenna is compared with the dual-sense CP and dual-band CPSIW antennas of [15]–[17]. It should be noted that the dual-band SIW antennas have the same sense of polarization at the bands, whereas the proposed antenna can provide the same sense of polarization as well as different sense of polarization. Moreover, it shows that the sense of polarization can be easily selected by a proper choice of the flare angle. The size of the proposed antenna is smaller than in [16] and [17]. The bands can be tuned independently, which is not shown in [16] and [17]. Since the antenna provides narrow CP beam width, it can be effectively used in point-to-point communication systems and in satellites and radar systems where highly directional beams are used.

REFERENCES

[1]. J. Y. Sze, C. I. G. Hsu, Z. W. Chen, and C. C. Chang, "Broadband CPW-fed circularly polarized square slot antenna with lightning-shaped feedline and inverted-L grounded strips," *IEEE Trans. Antennas Propag.*, vol. 58, no. 3, pp. 973–977, Mar. 2010.

[2]. R. K. Saini and S. Dwari, "A broadband dual circularly polarized square slot antenna," *IEEE Trans. Antennas Propag.*,

vol. 64, no. 1, pp. 290–294, Jan. 2016.

[3]. C. H. Chen and E. K. N. Yung, "Dual-band circularly-polarized CPW-fed slot antenna with a small frequency ratio and wide band widths," *IEEE Trans. Antennas Propag.*, vol. 59, no. 4, pp. 1379–1384, Apr. 2011.

[4]. W. Liang, Y. C. Jiao, Y. Luan, and C. Tian, "A dual band circularly polarized complementary antenna," *IEEE Antennas Wireless Propag. Lett.*, vol. 14, pp. 1153–1156, 2015.

[5]. X. L. Bao and M. J. Amman, "Monofilar spiral slot antenna for dual frequency dual sense circular polarization," *IEEE Trans. Antennas Propag.*, vol. 59, no. 8, pp. 3061–3065, Aug. 2011.

[6]. X. Bao and M. J. Amman, "Dual frequency dual sense circularly polarized slot antenna fed by micro stripline," *IEEE Trans. Antennas Propag.*, vol. 56, no. 3, pp. 645–649, Mar. 2008.

[7]. Y. Shao and Z. Chen, "A design of dual frequency dual sense circularly polarized slot antenna," *IEEE Trans. Antennas Propag.*, vol. 60, no. 11, pp. 4992–4997, Nov. 2012.

[8]. Y. Y. Chen, Y. C. Jiao, G. Zhao, F. Zhang, Z. L. Liao, and Y. Tian, "Dual band dual sense circularly polarized slot antenna with a C-shaped grounded strip," *IEEE Antennas Wireless Propag. Lett.*, vol. 10, pp. 915–918, 2011.

[9]. Z. X. Liang, D. C. Yang, X. C. Wei, and E. P. Li, "Dual band dual circularly polarized micro strip antenna with two concentric rings and an arc-shaped conducting strip," *IEEE Antennas Wireless Propag. Lett.*, vol. 15, pp. 834–837, 2016.

[10]. C. F. Jou, J. W. Wu, and C. J. Wang, "Novel broadband monopole antennas with dual-band circular polarization," *IEEE Trans. Antennas Propag.*, vol. 57, no. 4, pp. 1027–1034, Apr. 2009.

[11]. R. K. Saini, S. Dwari, and M. K. Mandal, "CPW-fed dual-band dual-sense circularly polarized monopole antenna," *IEEE Antennas Wireless Propag. Lett.*, vol. 16, pp. 2497–2500, 2017.

[12]. G. Q. Luo, Z. F. Hu, L. X. Dong, and L. L. Sun, "Planar slot antenna backed by substrate integrated waveguide cavity," *IEEE Antennas Wireless Propag. Lett.*, vol. 7, pp. 236–239, 2008.

[13]. S. Mukherjee, A. Biswas, and K. V. Srivastava, "Broadband substrate integrated waveguide cavity-backed bow-ties slot antenna," *IEEE Antennas Wireless Propag. Lett.*, vol. 13, pp. 1152–1155, 2014.

- [14]. G. Q. Luo, Z. F. Hu, Y. Liang, L. Y. Yu, and L. L. Sun, "Development of low profile cavity backed cross lotantennas for planar integration,"IEEE Trans.AntennasPropag.,vol.57,no.10,pp.2972–2979,Oct.2009.
- [15]. K. Kumar, S. Dwari, and M. K. Mandal, "Broadband dual circularly polarized substrate integrated wave guide antenna,"IEEEAntennasWireless Propag. Lett., vol. 16, pp. 2971–2974,2017.
- [16]. T. Zhang, W. Hong, Y. Zhang, and K. Wu, "Design and analysis of SIW cavity backed dual band antennas with a dual mode triangular ring slot," IEEE Trans. Antennas Propag., vol. 57, no. 10, pp. 5007–5016, Oct.2014.
- [17]. Q. Wu, J. Yin, C. Yu, H. Wang, and W. Hong, "Low-profile millimeter-wave SIW cavity-backed dual-band circularly polarized antenna," IEEE Trans.AntennasPropag.,vol.65,no.12,pp.7310–7315,Dec.2017.

Dr.Pravat Kumar Subudhi as, " A Circularly Polarized Substrate Integrated Waveguide Antenna " *International Journal of Engineering Research and Applications (IJERA)*, vol.5(8), 2015, pp 282-287.